

Serial Search Based Initial Code Acquisition in the Multiple Transmit/Receive Antenna Aided Multi-Carrier DS-CDMA Downlink

SeungHwan Won and Lajos Hanzo
 School of ECS, Univ. of Southampton, SO17 1BJ, UK.
 Tel: +44-23-8059 3125, Fax: +44-23-8059 4508
 E-mail: {shw04r, lh}@ecs.soton.ac.uk
 http://www-mobile.ecs.soton.ac.uk

Abstract—Initial code acquisition schemes designed for the multiple transmit/receive antenna aided Multi-Carrier (MC)-DS-CDMA downlink are analysed, when communicating over uncorrelated Rayleigh channels. The achievable Mean Acquisition Time (MAT) performance is characterised as a function of both the number of transmit/receive antennas and that of the number of subcarriers. It is demonstrated that in contrast to our expectations, the achievable MAT tends to degrade at low E_c/I_o values right across the Signal-to-Interference plus Noise Ratio (SINR) per chip (E_c/I_o) range considered, when the number of transmit antennas and/or that of the subcarriers are increased. An exception is constituted by Single-Carrier (SC)-DS-CDMA using $P = 2$ and 4 transmit antennas and $R=1$ receive antenna. This increased MAT has a grave detrimental effect on the performance of Rake receiver based synchronisation schemes, when the perfectly synchronised idealised system is capable of attaining its target bit error rate performance at reduced SINR values, as a benefit of the diversity gain achieved by employing both multiple transmit antennas and multiple subcarriers. Therefore our future research will be aimed at specifically designing powerful iterative acquisition schemes for MIMO-aided multi-carrier transmission systems.

I. INTRODUCTION

Employing multiple transmit antennas in the downlink of wireless systems constitutes an attractive technique of reducing the detrimental effects of time-variant multi-path fading environments [1]. Furthermore, exploiting multiple subcarriers in the downlink of wireless systems exhibits considerable benefits in terms of the achievable data throughput [2],[3]. The combination of Single-Carrier Code Division Multiple Access (SC) CDMA and Orthogonal Frequency Division Multiplexing (OFDM) has drawn substantial research attention [2]-[5]. In inter-cell synchronous CDMA systems the mobile station's (MS) receiver must be capable of synchronously aligning a locally generated pseudonoise (PN) code with the desired user's PN sequence which may be completely buried in CoChannel Interference (CCI). Substantial research efforts have been devoted to the design of code acquisition techniques for Single-Input Single-Output (SISO) systems [5], with the aim of minimising the Mean Acquisition Time (MAT) [5],[6]. The serial acquisition performance of Multi-Carrier (MC) DS-CDMA has been analysed in [7]. A serial search based code acquisition scheme was analysed in the context of the multiple transmit antenna aided SC-DS-CDMA downlink in [8]. **However, since no in-depth analysis of code acquisition schemes designed for a multiple transmit/receive antenna aided MC-DS-CDMA system is available in the literature, this is the objective of the present contribution.** Against this backdrop, we set out to analyse a serial search based initial code acquisition scheme designed for multiple transmit/receive antenna aided MC-DS-CDMA systems.

The financial support of the Ministry of Information and Communication(MIC), Republic of Korea and the European Union under the auspices of the Phoenix and Newcom projects and that of the EPSRC is gratefully acknowledged.

More explicitly, we quantify both the correct detection probability as well as the false alarm probability as a function of both the SINR per chip and that of the number of transmit/receive antennas as well as that of the number of subcarriers. Furthermore, we quantify the MAT versus E_c/I_o performance parameterised by both the number of transmit/receive antennas and that of the subcarriers.

This paper is organised as follows. Section II describes the system investigated, followed by the correct detection and false alarm probability analysis of serial-search based initial code acquisition schemes in the context of uncorrelated Rayleigh channels, whilst the MAT aspects of initial code acquisition designed for multiple transmit/receive antenna aided MC-DS-CDMA systems are briefly considered in Section III. In Section IV, our numerical MAT results are discussed, while our conclusions are offered in Section V.

II. CORRECT DETECTION AND FALSE ALARM PROBABILITY

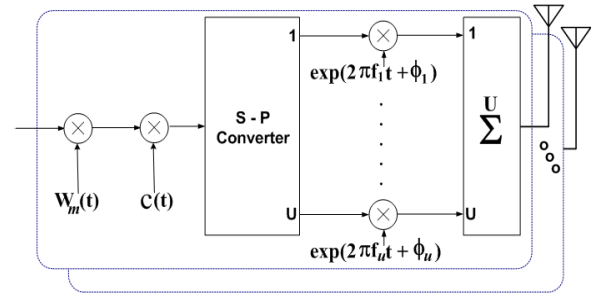


Fig. 1. Transmitter schematic of the MC-DS-CDMA downlink having P transmit antennas and U subcarriers.

Fig.1 portrays the transmitter schematic of the MC-DS-CDMA downlink having P transmit antennas and U subcarriers. In the MC-DS-CDMA system considered the input bit sequence is Serial-to-Parallel (SP) converted and each of the parallel sequences is transmitted on a separate subcarrier, as seen in Fig.1. The transmitted signal of the multiple transmit antenna assisted base station can be expressed as

$$S_{tot}(t) = \sum_{m=1}^P \sum_{u=1}^U \left[\sqrt{\frac{E_c}{PT_c}} b(t) c(t) w_m(t) \cdot \exp(2\pi f_u t + \phi_u) \right], \quad (1)$$

where $p = 1, \dots, P$ indicates the number of transmit antennas, $u = 1, \dots, U$ is the number of subcarriers, $b(t)$ represents the pilot data sequence assuming a value of binary '1' [9], $c(t)$ denotes the unique user-specific PN sequence, $w_m(t)$ identifies the specific Walsh code assigned to the p^{th} transmit antenna, E_c denotes the pilot signal energy per PN code chip, T_c indicates the chip duration, f_u

is the u^{th} subcarrier frequency, and ϕ_u denotes the u^{th} subcarrier phase of the modulator. Furthermore, T_b represents the bit duration of the data sequence before serial-to-parallel conversion, while T_s indicates the symbol duration after SP conversion. Accordingly, we have $T_s = U \cdot T_b$. The total allocated power is equally shared by the P transmit antennas. The spreading factor of the subcarrier signals in the MC-DS-CDMA system SF is T_s/T_c , while $SF_1 = T_b/T_{c1}$ denotes the spreading factor of a corresponding SC-DS-CDMA system, where T_{c1} denotes the chip duration of the corresponding SC-DS-CDMA signal. For the sake of simplicity we postulate in the forthcoming analysis that the main spectral lobes of two adjacent subcarriers do not overlap in the MC-DS-CDMA system considered here [7]. Furthermore, we assume that each subcarrier signal occupies an identical bandwidth and the total bandwidth is equally divided among the U number of subcarriers. Therefore, the following relationships hold $T_c = U \cdot T_{c1}$, $SF_1 = SF$ since $T_s = U \cdot T_b$. According to the above assumption, both the MC- and the corresponding SC-DS-CDMA systems have the same information rate of $1/T_b$ and the same bandwidth of $2/T_{c1}$, as suggested in [7], which allows their direct comparison in our forthcoming discourse.

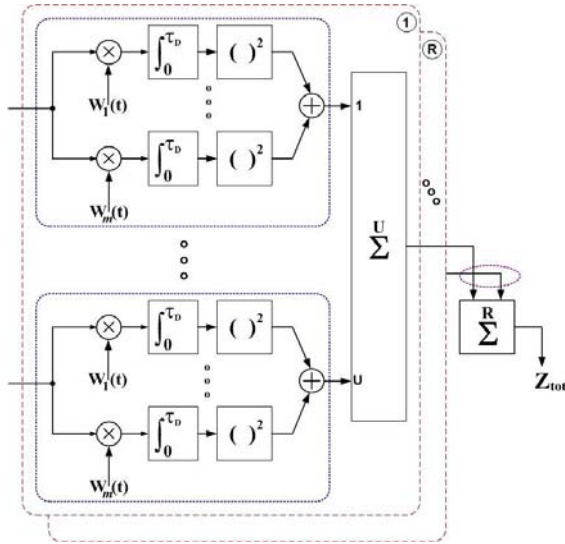


Fig. 2. Receiver structure of a noncoherent code acquisition system employing both R receive antennas and U subcarriers.

The received signal of the MIMO-aided noncoherent MC-DS-CDMA downlink may be expressed as

$$r_{tot}(t) = \sum_{m=1}^P \sum_{n=1}^R \sum_{u=1}^U [\alpha_{m,n,u} \sqrt{\frac{E_c}{PT_c}} c(t + dT_c) w_m(t + dT_c) \cdot \exp(2\pi f_u t + \phi_{(m,n,u)}) + I_{(m,n,u)}(t)], \quad (2)$$

where $n = 1, \dots, R$ is the number of receive antennas, $\alpha_{m,n,u}$ represents the envelope of the $(m, n, u)^{th}$ received signal path obeying the Rayleigh distribution, d is the code phase offset with respect to the phase of the local code and τ_D indicates the integral dwell time. Furthermore, $I_{(m,n,u)}(t)$ is the complex-valued Additive White Gaussian Noise (AWGN) having a double-sided power spectral density of I_0 , which contaminates the $(m, n, u)^{th}$ path. Fig.2 depicts the block diagram of the noncoherent receiver designed for our MC-DS-CDMA code acquisition scheme using multiple transmit/receive antennas, which generates a decision variable by accumulating

$(P \cdot R \cdot U)$ number of independently faded signals observed over a time interval. In the context of the receiver structure of Fig.2, the final decision variable may be expressed with the aid of the procedures suggested in [10] as follows

$$Z_k = \sum_{m=1}^P \sum_{n=1}^R \sum_{u=1}^U \left\| \frac{1}{\sqrt{2}} \cdot \left(\sqrt{\frac{4E_c}{NI_0P}} \cdot S_{k(m,n,u)} + I_{k(m,n,u)} \right) \right\|^2, \quad (3)$$

where k denotes the k^{th} chip's sampling instant, $S_{k(m,n,u)}$ is assumed to be deterministic as shown in [10], $\|\cdot\|^2$ represents the squared envelope of the complex-valued argument and $1/\sqrt{2}$ is a normalisation factor regarding the noise variance. Therefore, the decision variable Z_k obeying a noncentral chi-square PDF with $(2P \cdot R \cdot U)$ degrees of freedom has its noncentrality parameter λ_x , which is either $\frac{2N}{P}(\frac{E_c}{I_0})$, when it is deemed to be present ($x = 1$) or $\frac{2}{NP}(\frac{E_c}{I_0})$, when it is deemed to be absent ($x = 0$) [10], where the PDF is given by [11]

$$f_{Z_k}(z|H_x) = \frac{1}{2} \left(\frac{z}{\lambda_x} \right)^{\frac{(PRU-1)}{2}} \cdot \exp \left[-\frac{(z + \lambda_x)}{2} \right] \cdot \mathcal{I}_{(PRU-1)} \left(\sqrt{z \cdot \lambda_x} \right) \quad (4)$$

and where $z \geq 0$, $x = 0$ or 1 and $\mathcal{I}_{(PRU-1)}(\cdot)$ is the $(P \cdot R \cdot U - 1)^{st}$ -order modified Bessel function. It is worth mentioning that for SC-DS-CDMA, the coherent integration interval of N chip durations in the above formula should be substituted by $N_1 = NU$, since in this scenario $N_1 = \tau_D/T_{c1} = MU$ indicates the number of chips accumulated within the integral dwell time τ_D . For the sake of expressing the PDF conditioned on the presence of the desired user's signal in $f_{Z_k}(z|H_x)$ formulated for transmission over an uncorrelated Rayleigh channel, first the PDF $f_{Z_{k(m,n)}}(z|H_x, \beta)$ corresponding to a specific SINR β conditioned on the hypothesis of the desired signal being transmitted over an AWGN channel is weighted by the probability of occurrence $f(\beta)$ of encountering the SINR β , as quantified by the PDF. The resultant product is then averaged over its legitimate range of $-\infty \sim \infty$, yielding:

$$f_{Z_{k(m,n,u)}}(z|H_x) = \int_{-\infty}^{\infty} f(\beta) \cdot f_{Z_{k(m,n,u)}}(z|H_x, \beta) d\beta \quad (5)$$

$$= \int_0^{\infty} \left(\frac{e^{-\beta/\sigma^2}}{\sigma^2} \right) \cdot \frac{\exp[-(z + \beta\lambda_x)/2]}{2} \cdot \mathcal{I}_0 \left(\frac{2\sqrt{\beta\lambda_x z}}{2} \right) d\beta \quad (6)$$

$$= \frac{\exp[-z/(2 + \lambda_x\sigma^2)]}{(2 + \lambda_x\sigma^2)} \quad (7)$$

$$\equiv \frac{\exp[-z/(2 + \bar{\lambda}_x)]}{(2 + \bar{\lambda}_x)}, \quad (8)$$

where the definition of $(E_c/I_0)'$ [9] encompasses the effects of both timing errors and frequency mismatches and the corresponding noncentrality parameter, $\bar{\lambda}_x \equiv \lambda_x\sigma^2$ is either $\frac{2N}{P}(\frac{E_c}{I_0})'$ for the hypothesis of the desired signal being present ($x = 1$) or $\frac{2}{NP}(\frac{E_c}{I_0})'$ for it being absent ($x = 0$). We also define $\mu_x = (2 + \bar{\lambda}_x)$, which physically represents a new biased noncentrality parameter. Further details on the related calculations can be found in [9],[10]. Finally, we arrive at the PDF of $Z_{k(m,n,u)}$ conditioned the presence of the

desired signal in the form of:

$$f_{Z_k(m,n,u)}(z|H_x) = \frac{1}{\mu_x} e^{-z/\mu_x}. \quad (9)$$

Since the decision variable Z_k of Eq.3 is constituted by the sum of $(P \cdot R \cdot U)$ number of independent variables ($Z_k = \sum_{m=1}^P \sum_{n=1}^R \sum_{u=1}^U Z_{k(m,n,u)}$), which has a PDF given by Eq.9, we can derive the Laplace transform of each by raising them to the $(P \cdot R \cdot U)^{th}$ power and then performing the inverse transform in order to generate the resultant PDF [9], leading to:

$$f_{Z_k}(z|H_x) = \frac{z^{(PRU-1)} e^{-z/\mu_x}}{\Gamma(PRU) \cdot \mu_x^{PRU}}, \quad (10)$$

where $\Gamma(\cdot)$ is the Gamma function. Finally, the probability of correct detection or false alarm corresponding to $x = 1$ or 0 , respectively, is obtained as

$$P|_{x=1 \text{ or } 0} = \int_{\theta}^{\infty} f_{Z_k}(z|H_x) dz \quad (11)$$

$$= \exp\left(-\frac{\theta}{\mu_x}\right) \cdot \sum_{k=0}^{PRU-1} \frac{(\theta/\mu_x)^k}{k!}, \quad (12)$$

where θ is a threshold value. Given Eq.12, the transfer functions required for the sake of characterising the multiple antenna aided SC- and MC-DS-CDMA schemes can be readily derived [9],[12].

Before moving on to the next section, it is worth noting that the PN sequence chip duration T_{c1} of the SC-DS-CDMA signals is U times lower than that of the MC-DS-CDMA signals, namely, $T_{c1} = T_c/U$. This is because given the same allocated bandwidth and the same total transmitted energy per chip, the bandwidth of the SC-DS-CDMA signal is U times higher than that of the subcarrier signals in the MC-DS-CDMA system exploiting U subcarriers. Moreover, for the sake of maintaining a constant integral dwell time of τ_D , the chip energy accumulated by the SC-DS-CDMA receiver during the period of τ_D is U times higher than that collected by the MC-DS-CDMA correlator of each subcarrier, since the number of chips within the period of τ_D is U times higher for the SC-DS-CDMA system than that of the MC-DS-CDMA system [7].

III. MAT ANALYSIS OF CODE ACQUISITION

The family of serial search acquisition techniques [9] has been traditionally applied, where the search window width is quite wide, on the order of $(2^{15} - 1)$ chips. As a consequence, in the context of serial search achieving a low MAT constitutes the most critical performance criterion, as exemplified by the downlink of the inter-cell synchronous CDMA-2000 system [9],[12]. In initial code acquisition designed for SC-DS-CDMA, the main objective is to synchronise with the direct received signal path, corresponding to the reference finger of the Rake receiver.

The MAT of a single-antenna aided serial search based initial code acquisition scheme was analysed in [9],[12]. The main difference between a single-antenna and a multiple-antenna assisted MC-DS-CDMA system manifests itself in terms of deriving the correct detection and the false alarm probability as a function of both the number of the transmit/receive antennas and that of the subcarriers, both of which influence the attainable MAT. We will commence our discourse by analysing the MAT performance of an initial code acquisition scheme employing Double Dwell Serial Search (DDSS) [12]. We assume that in each chip duration T_c , l number of correct

timing hypotheses are tested, which are spaced by T_c/l . Hence the total uncertainty region is increased by a factor of l . All the resultant $(\nu - 2l)$ states that may lead to a false alarm are expected to increase the MAT as a function of the associated penalty time which corresponds to the time required for the system to revert back to its search mode, since it was taken by declared that it identified the perfectly synchronised state. The $2l$ legitimate locking states within a lag of one chip duration of the correct timing instant are considered in the MAT analysis. The required transfer functions [12] are defined as follows. The function $H_D(z)$ includes all branches of a state diagram [12] leading to successful detection, $H_0(z)$ denotes the absence of the desired user's signal at the output of the code acquisition scheme, whilst $H_M(z)$ indicates the probability of failing to detect the correctly synchronised code-phase during a search run carried out across the entire uncertainty region. These definitions are detailed in [12] for DDSS. Then, it may be inferred that the generalised expression derived for calculating the MAT of the serial search based initial code acquisition scheme is given by [9],[12]:

$$E[T_{ACQ}] = \frac{1}{H_D'(1)} [H_D'(1) + H_M'(1) + \{(\nu - 2l)[1 - \frac{H_D(1)}{2}] + \frac{1}{2}H_D(1)\}H_0'(1)] \cdot \tau_{D1}, \quad (13)$$

where $H'_x(z)|_{x=D, M \text{ or } 0}$ is a derivative of $H_x(z)|_{x=D, M \text{ or } 0}$ and τ_{D1} represents the 1st dwell time.

IV. NUMERICAL SYSTEM PERFORMANCE RESULTS

In this section we will characterise the MAT performance of the multiple transmit/receive antenna aided MC-DS-CDMA code acquisition scheme of Fig.2. Our performance comparison between the SC-DS-CDMA system ($U = 1$) and various MC-DS-CDMA ($U = 2$ and 4) systems using different number of subcarriers is based upon the assumptions that these systems support the same total transmission rate and employ the same total transmitted energy per chip. Furthermore, it is assumed that the integral dwell time, τ_D , is the same for all the scenarios considered here. In Table 1 we outlined the maximum SINR degradation imposed by both the Doppler shift and the frequency mismatch between the transmitter and receiver in conjunction with the coherent integration interval of N chip durations, seen in Fig.2 for the initial code acquisition. The length of the PN sequence in our system was assumed to be $(2^{15} - 1) \cdot T_c$, where the chip-durations employed here for $U = 1, 2$ and 4 are $T_{c1} = 1/2.4576\mu s$, $T_c = 1/1.2288\mu s$ and $T_c = 1/0.6144\mu s$, respectively. In the case of the initial code acquisition scheme of Fig.2, the number of chips over which the accumulator Σ of Fig.2 sums the $(\cdot)^2$ envelope detector's output in both the search and the verification modes of DDSS are assumed to be 128 and 512 in the SC scheme of $U = 1$, 64 and 256 in the $U = 2$ MC-DS-CDMA arrangement, as well as 32 and 128 in the $U = 4$ scenarios, respectively. These optimised parameter values were calculated by using both Eq.12 and Eq.13 as well as Eq.(3.7) of [9] provided for determining the performance degradation owing to both the Doppler shift and the frequency mismatch. The spreading factor of the Walsh code to be acquired was selected to be 128. The frequency mismatch was assumed to be 1000Hz for the initial code acquisition [9], while the carrier frequency was 1.9GHz. The corresponding relative difference was $10^3/(1.9 \times 10^9) \approx 5 \times 10^{-7}$. As a worst-case mobile speed, it is reasonable to postulate 160 km/h. We also assumed that the sampling inaccuracy caused by having a finite, rather than infinitesimally low search step size of $\Delta = 1/2T_c$

was -0.91dB, which is a typical value for the search step size [9],[12]. The total uncertainty region of initial code acquisition was assumed to entail 65534 hypotheses. Finally, in the spirit of [13], the false locking penalty factor was assumed to be 1000. For simplicity, it was assumed that only a single received signal path is encountered in a given search window. All the performance curves have been obtained at the threshold value of $E_c/I_o = -16dB$, which was experimentally designed for the initial code acquisition scheme.

Fig.3 characterises the MAT versus SINR per chip performance of DDSS for the initial code acquisition arrangement of the SC-DS-CDMA benchmark system as a function of the number of transmit antennas for $P = 1, 2$ as well as 4 and that of the number of receive antennas for the specific values of $R = 1, 2$ and 4. As the number of transmit antennas is decreased, all the curves seen in Fig.3 illustrate an improved MAT performance of the systems exploiting $R = 2$ and 4 receive antennas, except for the $R = 1$ scenarios over the specific SINR range shown in Fig.3. To illustrate the above fact a little further, in the cases of both ' $P2R1$ ' and ' $P4R1$ ' the DDSS scheme exhibits a better MAT performance in comparison to the ' $P1R1$ ' arrangement across the specific SINR range considered. In other words, this clearly implies that the DDSS scheme employing $R = 1$ receive antenna benefits from a higher diversity gain in the SC-DS-CDMA scenario. However, the performance degradation imposed by employing multiple antennas becomes more drastic in the low SINR range, as the number of transmit antennas is increased in the DDSS-aided initial code acquisition scenario. In case of employing both multiple transmit and multiple receive antennas, similar trends are observable, although using two or four receive antennas has the potential of mitigating the associated acquisition performance degradation imposed by the low per-branch E_c/I_o values associated with the employment of multiple transmitters.

Fig.4 and 5 illustrate the achievable MAT versus SINR per chip performance of the DDSS-aided MC-DS-CDMA initial code acquisition scheme parameterised with both the number of transmit and receive antennas, when using $U = 2$ and 4 subcarriers, respectively. In the case of the MC-DS-CDMA system, these schemes benefit for a predefined inherent diversity order determined by the number of subcarriers used. It is also assumed that the total transmitted energy per chip is the same in all the scenarios considered. Accordingly, the effect of the inherent frequency diversity is the same as that of the multiple transmit antenna aided diversity, as documented in [8]. This fact clearly indicates that employing multi-carrier transmissions based on the DS-CDMA principle leads to exactly the same detrimental impact on the achievable MAT performance as that caused by employing the multiple transmit antennas. For the sake of a fair comparison, the maximum diversity order considered in Fig.4 and 5 is limited to 16. The results of Fig.4 are parameterised by both the number of transmit antennas for $P = 1, 2$ as well as 4 and by the number of receive antennas for $R = 1$ as well as 2. Similarly, the results of Fig.5 are parameterised by both the number of transmit antennas for $P = 1$ and 2 as well as by the number of receive antennas for $R = 1$ and 2. As both the number of transmit antennas and that of the subcarriers is decreased, all the curves seen in both Fig.4 and Fig.5 indicate an improved MAT performance. This trend explicitly illustrates that the DDSS-aided MC-DS-CDMA initial acquisition scheme degrades the achievable MAT performance of SC-DS-CDMA as a consequence of both the low per-antenna power imposed by employing multiple transmit antennas for the sake of attaining either a transmit diversity gain or an increased throughput and the low per-

subcarrier power imposed by using multiple subcarriers for the sake of achieving a frequency diversity gain. To interpret the above results a little further, a low level of both per-branch and per-subcarrier received signal strength would lead to a low acquisition performance, despite achieving a high transmit and frequency diversity gain. In other words, a high transmit and frequency diversity order effectively results in an acquisition performance loss, as a consequence of the insufficiently high signal strength per both transmit antenna branch and subcarrier branch.

Fig.6 documents the relationship between the SINR per chip required by the DDSS-aided initial code acquisition scheme for approaching their lowest possible MAT versus the number of subcarriers ($U = 1, 2$ and 4) parameterised with both the number of transmit and receive antennas. More explicitly, for $R = 1$ and $R = 2$ receive antennas, the required E_c/I_o values are compared at MAT = 6 and 4 seconds, respectively. As either the number of transmit antennas or the number of subcarriers is increased, the value of the required E_c/I_o is also increased, except for the ' $P1R1$ ' scenario, benefiting from the positive effect of the increased frequency diversity gain. It is also worth mentioning that according to Fig.6 the required E_c/I_o value tends to increase, as the number of subcarriers is increased, on provided that there exists no spectral overlap between the spectral main lobes of two adjacent subcarriers in the MC-DS-CDMA system considered [7]. Since the reliable operational range in the verification mode of the DDSS-aided initial code acquisition scheme is a false alarm probability spanning from 10^{-3} to 10^{-4} , as the number of subcarriers is increased, the correct detection probability considerably decreases according to the relationship between the correct detection versus false alarm probability formulated in Eq.12.

V. CONCLUSION

In this treatise, we analysed the multiple antenna aided transmit/receive diversity effects on the performance of the initial code acquisition scheme of the inter-cell synchronous MC-DS-CDMA downlink. The probabilities of correct detection and false alarm have been derived analytically and numerical results were provided in terms of the attainable MAT performance. Unexpectedly, our results suggest that increasing both the number of transmit antennas and that of the subcarriers in a MIMO-aided MC-DS-CDMA system results in combining the low-energy, noise-contaminated signals of both the transmit antennas and the subcarriers, which may degrade the MAT by an order of magnitude, when the SINR is relatively low. This phenomenon imposes a grave degradation on the performance of Rake receiver aided initial code acquisition schemes, when the perfectly synchronised idealised system is capable of attaining its target bit error rate performance at reduced SINR values, as a benefit of exploiting both multiple transmit antennas and frequency diversity. Hence our future research will be focused on specifically designing iterative turbo acquisition schemes [5] for MIMO-aided multi-carrier transmission systems.

REFERENCES

- [1] D. Gesbert, M. Shafi, D.S. Shiu, P.J. Smith, and A. Nguib, From Theory to Practice: An Overview of MIMO Space-Time Coded Wireless Systems, IEEE Journal on Selected Areas in Communications, vol. 21, NO.3, Issue 3, 2003, pp281-302.
- [2] S. Hara, R. Prasad, Overview of Multicarrier CDMA, IEEE Communications Magazine, Vol. 35, NO.6 Issue 12, 1997, pp126-133.
- [3] L-L Yang, L. Hanzo, Multicarrier DS-SS-CDMA: A Multiple Access Scheme for Ubiquitous Broadband Wireless Communications, IEEE Communications Magazine, Vol. 41, NO.10 Issue 10, 2003, pp116-124.

- [4] L-L. Yang, L. Hanzo, Performance of Generalized Multicarrier DS-CDMA over Nakagami-m Fading Channels, IEEE Transactions on Communications, vol. 50, NO.6, Issue 6, 2002, pp956–966.
- [5] L. Hanzo, L-L. Yang, E-L. Kuan, K. Yen, Single- and Multi- Carrier DS-CDMA, IV Multi-Carrier CDMA, Wiley, 2003.
- [6] B-G Lee, B-H Kim, Scrambling Techniques For CDMA Communications, Chapter 2 and 3, Kluwer Academic Publishers, 2001.
- [7] L-L. Yang, L. Hanzo, Serial Acquisition Performance of Single-Carrier and Multicarrier DS-CDMA over Nakagami-m Fading Channels, IEEE Transactions on Wireless Communications, vol. 1, NO.4, Issue 4, 2002, pp692–702.
- [8] S.H. Won, L. Hanzo, Analysis of Serial Search Based Code Acquisition in the Multiple Transmit Antenna Aided DS-CDMA Downlink, Vehicular Technology Conference, 2005, vol. 1, 25-28 September 2005, pp98–102.
- [9] A.J. Viterbi, CDMA: Principles of Spread Spectrum Communication, Chapter 3, Addison-Wesley, 1995.
- [10] J-C Lin, Differentially Coherent PN Code Acquisition with Full-Period Correlation in Chip-Synchronous DS/SS Receivers, IEEE Transactions on Communications, vol. 50, NO.5, Issue 5, 2002, pp698–702.
- [11] J.G. Proakis, Digital Communications, 3rd ed. Chapter 2, McGraw-Hill, 1995.
- [12] H-R Park and B-J Kang, On Serial Search Code Acquisition for Direct-Sequence Spread Spectrum System: An Application to IS-95 CDMA System, Vehicular Technology Conference, 1995, vol. 1, 25-28 July 1995, pp291–295.
- [13] H.R. Park, Performance Analysis of a Double-Dwell Serial Search Technique for Cellular CDMA Networks in the Case of Multiple Pilot Signals, IEEE Transactions on Vehicular Technology, vol. 48, NO.6, Issue 6, 1999, pp1819–1830.

TABLE I

MAXIMUM SINR DEGRADATION INFLICTED BY BOTH THE DOPPLER SHIFT AND A 1000HZ FREQUENCY MISMATCH IN COMPARISON TO A STATIONARY RECEIVER HAVING NO FREQUENCY DRIFT FOR THE COHERENT INTEGRATION INTERVAL OF N CHIP DURATIONS AT A CARRIER FREQUENCY OF 1.9GHz AS A FUNCTION OF THE NUMBER OF SUBCARRIERS ($U = 1, 2$ AND 4)

N(Chips): $U=1$	128	256	512	768	1024
N(Chips): $U=2$	64	128	256	384	512
N(Chips): $U=4$	32	64	128	192	256
Degradation(dB)	0.061	0.2449	0.9969	2.3144	4.3213

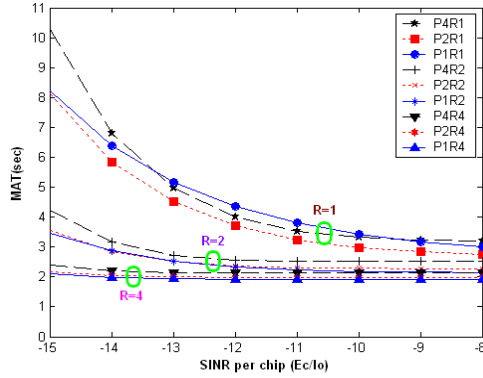


Fig. 3. MAT versus SINR per chip performance of the DDSS-aided SC-DS-CDMA initial code acquisition scheme parameterised with both the number of transmit and receive antennas.

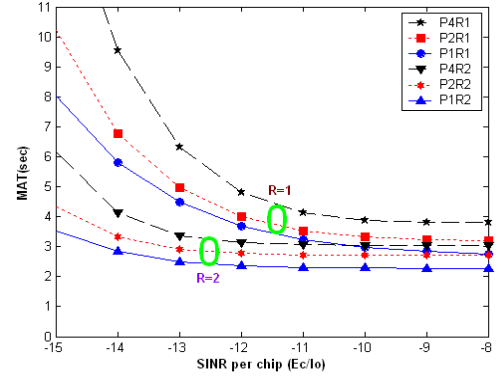


Fig. 4. MAT versus SINR per chip performance of the DDSS-aided MC-DS-CDMA initial code acquisition scheme parameterised with both the number of transmit and receive antennas for $U = 2$ subcarriers.

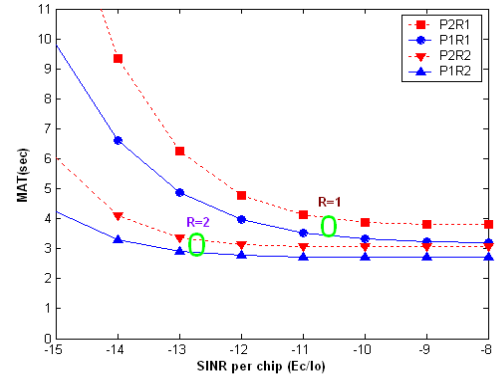


Fig. 5. MAT versus SINR per chip performance of the DDSS-aided MC-DS-CDMA initial code acquisition scheme parameterised with both the number of transmit and receive antennas for $U = 4$ subcarriers.

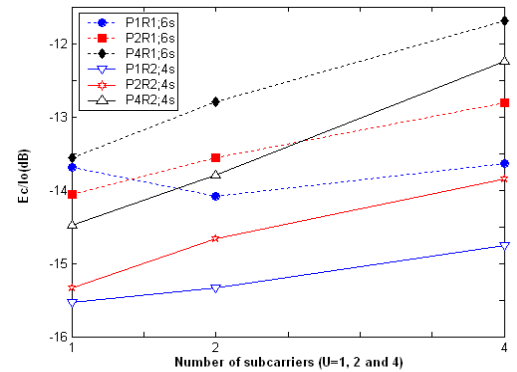


Fig. 6. SINR per chip performance versus the number of subcarriers ($U = 1, 2$ and 4) of the DDSS-aided MC-DS-CDMA initial code acquisition scheme parameterised with both the number of transmit and receive antennas.